Available online at www.sciencedirect.com
ScienceDirect
Bioelectrochemistry 70 (2007) 134 – 140
Bioelectrochemistry
www.elsevier.com/locate/bioelechem

On the temperature dependence of the dielectric membrane properties of human red blood cells

Jutiporn Sudsiri [1], Derk Wachner, Jan Gimsa *

University of Rostock, Institute of Biology, Gertrudenstr. 11A, D-18051 Rostock, Germany

Received 22 July 2005
Available online 5 April 2006

Abstract

Electrorotation (ER) spectra of human red blood cells (HRBCs) have been recorded in the frequency range from 10 kHz to 250 MHz in a 4-electrode microchip chamber. The cells were suspended at conductivities in the range from 0.02 to 3.00 S/m (corresponding to an ionic strength range from 1.6 to 343 mM) at temperatures between 10 °C and 35 °C. Generally, the characteristic frequencies as well as the rotation speeds of the first (membrane-dispersion) and second ER peaks increased with temperature. The rotation speed increase was largely correlated to the temperature dependence of the medium viscosity. Standard temperature dependencies were assumed for the conductivities and permittivities of cytoplasm, membrane, and external solution to explain the frequency shifts, starting from the cell parameters of Gimsa et al. [Gimsa et al., 1996, Biophys. J. 71: 495–506.]. The membrane capacitance was assumed to be temperature independent, based on the permittivity of alkyl-chains. Under these assumptions, the spectra could be well fitted only in a narrow temperature range around 20 °C. The temperature dependence of the first characteristic frequency was much stronger than predicted. In addition, around 15 °C, an anomalously high rotation speed was observed for the first peak at low external conductivities. Interestingly, this finding corresponds to the change in the chloride transport rate described by Brahm [Brahm, 1977, J. Gen. Physiol. 70: 283–306.].

Keywords: Electrorotation; Erythrocytes; Electric cell parameters; Cytoplasmic ion mobility; Membrane capacitance

1. Introduction

Electrorotation (ER) allows for investigating the dielectric properties of single biological cells. Cells are suspended in electrolyte medium and exposed to a rotating electric field for measurements. The field induces a rotating dipole moment in the cell. It consists of a component that is in-phase to the external field (real part) and a component out-of-phase to the external field (imaginary part). The components depend on the relative polarizability of cell and medium for a given field frequency. The interaction of the out of phase part of the induced dipole moment with the external field leads to a torque which can be observed microscopically as the rotation of individual cells. Theoretically, the torque is given by the cross product of the induced dipole moment of the cell and the external field, i.e. the product of the magnitudes of the imaginary part of the induced dipole moment and the external field. We modelled the HRBC as a conductive, oblate spheroid with a thin, insulating outer shell for the membrane. If the electric properties of the external medium are known, the electric properties, i.e. conductivities and permittivities of the model, can be inferred from the cell rotation spectra [1–4]. The reliability of the cell parameters can be improved by a combination of ER with other AC-electrokinetic methods [1,2].

In all techniques, membrane polarization is the major contribution to the cell dipole moment at low frequencies. The out-of-phase part of the external field will generate a torque when the time constant of membrane polarization introduces a phase-lag between the cell dipole moment and the external field. The frequency dependence of the magnitude of the out-of-phase part of the dipole moment forms a rotation peak that typically is of a Lorentzian shape. Such peaks can be described by the parameters characteristic frequency and peak height such as f_{c1} and R_1 for the

* Corresponding author. Tel.: +49 381 494 2037; fax: +49 381 494 2039.
E-mail address: jan.gimsa@uni-rostock.de (J. Gimsa).
[1] On leave from Prince of Songkla University, Department of Science and Techonology, Suratthani Campus, Muang, Suratthani 84100, Thailand.

1567-5394/$ - see front matter © 2006 Elsevier B.V. All rights reserved.
doi:10.1016/j.bioelechem.2006.03.010

Table 1
Electric cell parameters for 23 °C (bold) obtained from [3] were extrapolated according to Eq. (1)

Parameter	10 °C	15 °C	20 °C	23 °C [3]	25 °C	30 °C	35 °C
External permittivity	83.8	82.0	80.2	**79.1**	78.5	76.6	74.8
Membrane permittivity (for temperature dependence see text)	9.04	9.04	9.04	**9.04**	9.04	9.04	9.04
Internal permittivity before	224.5	219.7	214.9	**212.0**	210.1	205.2	200.3
and after dispersion (or no dispersion)	53.0	51.8	50.7	**50.0**	49.5	48.4	47.2
Dielectric decrement	171.5	167.9	164.2	**162.0**	160.6	156.8	153.1
Range of the external conductivity (S/m)	0.018–2.400	0.016–2.700	0.020–3.000	**0.001–1.390**	0.022–3.400	0.024–3.600	0.026–3.900
Membrane conductance ($\mu S/m^2$)	355.2	20.0	451.2	**480.0**	499.2	547.2	595.2
Internal conductivity before	0.301	0.342	0.376	**0.400**	0.416	0.456	0.496
and after dispersion (or no dispersion) (S/m)	0.409	0.457	0.506	**0.535**	0.554	0.603	0.652

Starting and end values of the relative permittivity and conductivity of the dispersive cytoplasm (Eq. (7)) were assumed to depend on temperature. In our model, these values were assumed not to dependent on the dispersion width. The "no dispersion" data were also used in a model with frequency independent parameters (compare to Figs. 3 and 4). These parameters largely coincide with those given for around 100 MHz in [19].

first, membrane-peak. The first peak is mainly determined by the membrane properties [5]. At higher frequencies, when the membrane is electrically transparent, the cellular polarization mainly arises from differences between cytoplasmic and external medium properties. A second ER peak (defined by f_{c2} and R_2) can be observed. It is caused by a transition of the polarization balance of the external and cytoplasmic media with increasing frequency. Whereas this balance is determined by the media conductivities at lower frequencies, it is determined by the permittivities at frequencies above the dispersion. Accordingly, the second peak of ER yields information on the properties of the cytoplasm.

Recently, ER experiments could be extended to the physiological [3,4] or even higher ionic strengths of the external medium [8]. These developments are based on microelectrode chambers allowing for the application of lower driving voltages and high medium conductivities. Usually, ER experiments are carried out at room temperature assuming the cell and medium parameters to be temperature independent [6,7]. Nevertheless, Joule's heating cannot be avoided. Heat production is linearly related to the electric conductivity and the square of the applied voltage [9]. A temperature increase by ΔT affects the viscosity, η, of the external medium, the permittivities, ε, and the conductivities, σ, of the system in the following ways:

$$\eta = \eta_{T_0} e^{-a\Delta T}, \varepsilon = \varepsilon_{T_0}(1-b\Delta T),\ \ \sigma = \sigma_{T_0}(1+c\Delta T) \tag{1}$$

with η_{T_0}, ε_{T_0}, and σ_{T_0} standing for the viscosity, permittivity and conductivity at temperature T_0. For values of ε_{T_0} and σ_{T_0}, see Table 1 The η_{T_0} values were obtained from measurements. The temperature coefficients a and c were assumed to be 0.02 K^{-1} for all media, whereas b has been extrapolated to 0.0046 K^{-1} for the external and internal media from the temperature dependence of the water permittivity [10,11].

Many authors have addressed the temperature effects on the physiology of HRBCs (see for example [12,13]). Temperature alterations will not only affect the cell dielectric properties of all phases but also the ion transport across the membrane. For example, a change of the chloride transport rate has been described around 15 °C presumably due to a change in the activation energy of the transport step [12]. Anion transport is mediated by the band-3 protein. With about 1.2×10^6 copies per cell it is the most abundant membrane protein in HRBCs. It is responsible for the fast anion exchange, and assumed to contribute to the membrane dielectric properties. If the protein's properties are altered, e.g. by inhibitors or a change in the temperature, the membrane properties will be changed. For example, the membrane capacity and conductivity have been found to increase and decrease, respectively, after the cells were incubated with the band 3 inhibitor 4,4′-diisothiocynostilbene-2,2′-disulphonate (DIDS) [7].

In this paper, we present results from ER measurements in the temperature range from 10 °C to 35 °C. For interpreting the experimental data, we assumed temperature dependent parameters starting from the cell parameters given in [3] for 23 °C. The parameters were introduced in the single shell model given in [5].

2. Theory

The rotation speed of a cell, is determined by the equilibrium of hydrodynamic friction T_{fric} and ER torque T_{ER}. Stoke's friction law for an oblate spheroid of axes ratio $a/b/c$=2:2:1 rotating around axis c at ω_c under laminar flow conditions is given by [14]:

$$T_{\text{fric}} = 5.64\pi\eta a^3\omega_c \tag{2}$$

Please note that the axis ratio has been derived from the electric cell data [3]. The more realistic ratio of $a/b/c$=3:3:1 would result in a coefficient of 4.88. Nevertheless, Eq. (2) does not take the surface friction into account that will increase for more oblate shapes. The ER torque is proportional to the cell volume, the square of the electric field strength E, and the imaginary part of the Clausius-Mossotti factor K^* (for the definition of K^* please refer to [5]):

$$T_{\text{ER}} = \frac{4\pi a^2 c}{3}\varepsilon_0\varepsilon_e E^2 \text{Im}(K^*) \tag{3}$$

ε_0 and ε_e are the permittivity of vacuum and the relative permittivity of the external medium, respectively. The asterisk marks the complex Clausius-Mossotti factor. Usually, the external field strength in the center of a four-electrode ER chamber is calculated from the applied voltage and the electrode tip distance. Nevertheless, the actual field strength is always lower than this. For our micro-chip design (Fig. 1), the field strength in the center of the chamber is E=0.806V/x, with V and x standing for the electrode voltage and tip-to-tip distance, respectively [15]. Another correction must be introduced for the

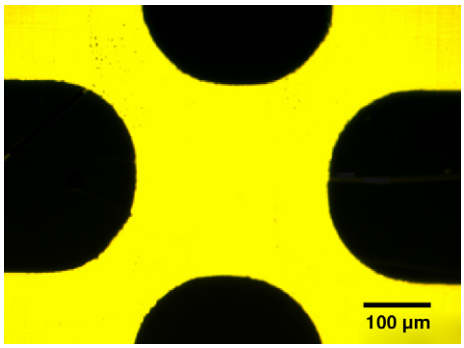

Fig. 1. Microchip electrode chamber with an electrode tip-to-tip distance of about 300 µm.

effect of the square topped measuring field on the induced torque. The higher harmonics result in a frequency dependent reduction of the torque in such fields [16]. The actual torque is reduced by a factor of 0.92 for well separated peaks. Then the rotation speed ω_c is derived for $T_{\text{fric}}=T_{\text{ER}}$:

$$\omega_c = \frac{T_{\text{ER}}/0.92}{5.64\pi\eta a^3} = 0.167\frac{\varepsilon_0\varepsilon_e c\ \text{Im}(K^*)E^2}{a\eta} \tag{4}$$

Along semiaxis a the Clausius-Mossotti factor is given by [5]:

$$K_a^* = \frac{a_{\text{inf}}}{a_{\text{inf}}-a}\left(1-\frac{Z_a^{\text{i}}+Z^{\text{m}}}{Z_a^{\text{i}}+Z^{\text{m}}+Z_a^{\text{e}}}\frac{a_{\text{inf}}}{a}\right) \tag{5}$$

for a spheroidal cell with a thin membrane. The impedance components for the cytoplasm (Z^{i}), the membrane (Z^{m}) and the external medium (Z^{e}) are given by:

$$Z_a^{\text{i}} = a/(\sigma_i + j\omega\varepsilon i\varepsilon_0), Z^{\text{m}} = d/(\sigma_m + j\omega\varepsilon_m\varepsilon_0), Z_a^{\text{e}} = (a_{\text{inf}}-a)/(\sigma_{\text{e}} + j\omega\varepsilon_{\text{e}}\varepsilon_{\text{e}}) \tag{6}$$

with a, a_{inf}, d and j standing for the length of semiaxis a, the influential radius in a-direction, the membrane thickness, and

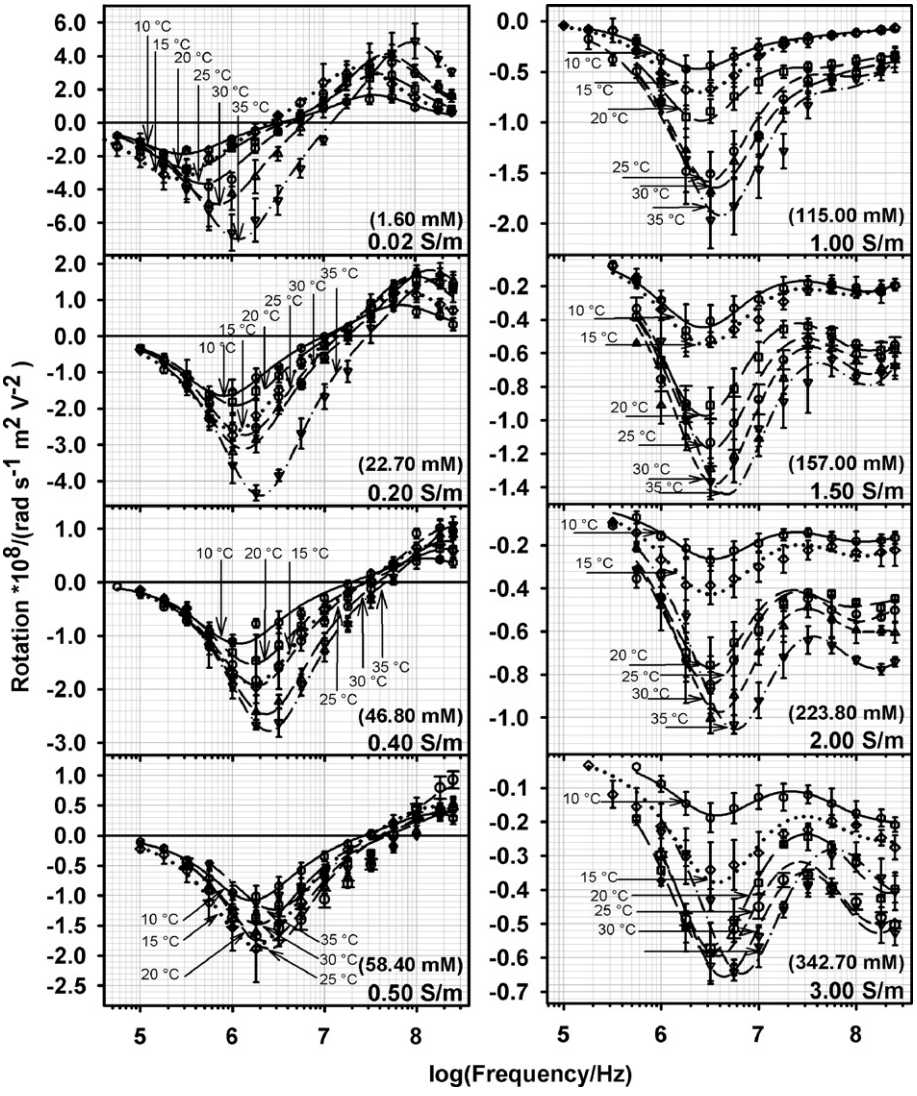

Fig. 2. ER spectra for various different external conductivities at six different temperature classes, 10 °C (hexagons, solid lines), 15 °C (diamonds, dotted lines), 20 °C (squares, long dash lines), 25 °C (circles, medium dash lines), 30 °C (triangles up, short dash lines), and 35 °C (triangles down, dash-dot lines). The conductivities given in the figures refer to 20 °C. The data in parentheses are the corresponding ionic strengths of the solutions. The spectra were measured in square-topped fields. Two superimposed Lorentzian peaks of the general form $2Rff_c/(f^2+f_c^2)$ were fitted to the measuring points. R, f and f_c stand for peak rotation speed, field frequency, and characteristic frequency, respectively. E was assumed to be V/x. The correction factor 0.806 was introduced in Eq. (4).

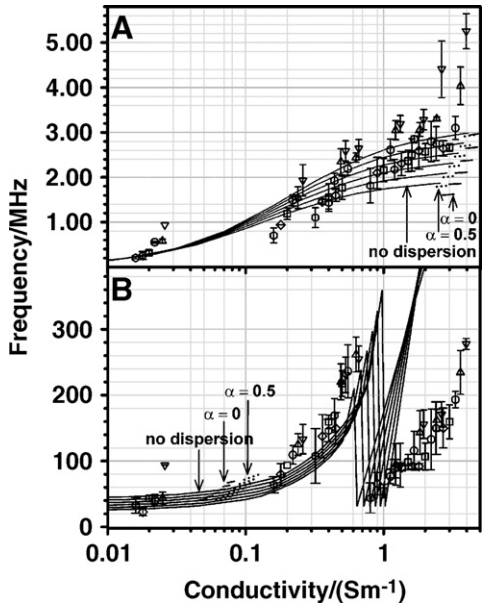

Fig. 3. First (A) and second (B) characteristic frequencies of Fig. 2 over external conductivity for different temperatures (for symbols see Fig. 2). Please note that all frequencies were divided by a factor of 1.066 to correct for the square wave measuring field (for details see [16]). The theoretical curves were calculated according to the temperature dependent parameters given in Table 1. Frequency independent parameters were assumed for the full curves. For comparison, the position of the curves with frequency dependent parameters is marked by short continuous and dotted lines. The dispersion-width α is marked in the figure (see Eq. (7)).

$(-1)^{0.5}$, respectively [5]. In the following, membrane conductance and membrane capacitance were calculated assuming a membrane thickness d of 8 nm.

We assumed the oblate cell model given in [5] with a long semiaxis of a=3.3 μm for HRBCs. An influential radius a_{inf}= 4.0 μm was obtained for an axis ratio of 1:2 [5]. The relative external permittivity, the membrane conductance, and the membrane capacitance were assumed to be 79.1, 480 S/m^2, and 9.97 mF/m^2, respectively, at 23 °C [3]. Low frequency values of 0.4 S/m and 212, dispersing around 15 MHz, were assumed for the conductivity and the relative permittivity of the cytoplasm. The dispersion leads to a relative permittivity of 50 and a conductivity of 0.535 S/m at high frequencies [3].

3. Materials and methods

3.1. Preparation of the cell suspension

Two 300 mosM solutions, a sucrose and a NaCl solution both containing 1 mM phosphate buffer (pH 6) were mixed to adjust the medium conductivity in the range from 0.02 S/m to 3.00 S/m. The conductivity of the suspension was measured in the temperature compensation mode (20 °C) with an InoLab-conductometer (WTW, Weilheim, Germany). Conductivities below 0.1 S/m were measured with a LF 39 (Sensortechnik Meinsberg GmbH, Meinsberg, Germany). The viscosities of all measuring solutions were determined by a falling-ball viscosimeter MLW (VEB MLW Prüfgerätewerk Medingen, Freital, GDR). 10 ml of the solution were equilibrated to the desired temperature by a thermostat prior to the suspension of fresh blood at a volume concentration (hematocrit) of 0.02% for each experiment. 5 μl of this suspension was transferred to the measuring chamber. The temperature of the chamber was controlled by a small thermistor.

3.2. ER measurements

The measuring chamber was based on a rectangular glass microchip with 4 platinum electrodes (Fig. 1) [2,8].

Rotating electric fields in the range from 50 kHz to 250 MHz were generated by application of four progressively 90°-phase shifted signals of a peak-to-peak voltage of 5 V_{PP} from a radio-frequency generator HP 8131A (Hewlett Packard, USA). ER spectra of 4–6 different cells were recorded via a video system at every conductivity. At conductivities above 2.00 S/m and 25 °C no complete spectra could be recorded on a single cell due to medium convections. Therefore, a new cell suspension was transferred to the chamber for every measuring point. All measurements were finished within 5 min after cell suspension. The obtained spectra were fitted by a function consisting of two Lorentzian peaks, corresponding to the two major ER peaks [1].

3.3. DIDS treatment

Experiments with the band 3 inhibitor DIDS (Sigma, Steinheim, Germany) were conducted at a concentration of 20 μM [17]. DIDS was added before suspending the HRBCs.

4. Results

Fig. 2 shows ER spectra for six different temperature classes measured in eight selected solutions with conductivities ranging from 0.02 S/m to 3.00 S/m. A linear temperature dependence

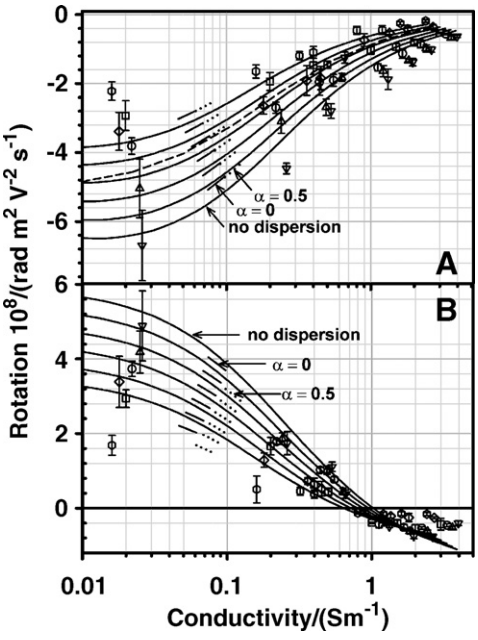

Fig. 4. Rotation peak amplitudes of the first (A) and second (B) peak obtained from the spectra fits of Fig. 2. For symbols and line types please see Fig. 3. An additional curve (dashed line) is given for the first peak at 15 °C assuming a reduced membrane conductance of 20 S/m^2 (see Discussion).

was measured for all solutions (cp. to Eq. (1) and to Figs. 3 and 4). At low and medium conductivities (0.02–0.50 S/m), co- and anti-field rotation peaks were clearly visible. Starting at 1.00 S/m also the second peak changed to negative. A strong shift of f_{c1} towards higher frequencies was observed for conductivities higher than 2.00 S/m at 30 °C and 35 °C. Nevertheless, changes in temperature did not alter the overall shape of the ER spectra ([18], see also Figs. 2 and 3).

An anomalous increase in the rotation speed was observed for low and medium conductivities at 15 °C (see Fig. 4A). We compared the ER spectra of control HRBCs and cells treated with DIDS to test whether this behavior is related to an alteration in the anion transport, mediated by the anion exchange protein band 3 (capnophorin). DIDS treatment lead to an increase in the rotation speed (magnitude of R_1, Fig. 5). No increase was observed only at 15 °C.

5. Discussion

5.1. Electric cell properties

Table 1 presents the temperature dependent parameters used to derive the theoretical curves in Figs. 3 and 4. Frequency independent as well as cell parameters for a dispersive cytoplasm have been taken from [3]. Temperature dependencies according to Eq. (1) have been used to calculate the permittivities and conductivities for temperatures deviating from 23 °C. No temperature dependence has been assumed for the membrane permittivity since the temperature coefficients for the permittivities of fatty acid-chain-like compounds are very low [11]. The frequency dependent transitions of the cytoplasmic permittivity and conductivity have been described according to the dispersion relation by the following phenomenological equations [3]:

$$\varepsilon_i = \varepsilon_i^{\infty} + \Delta\varepsilon \frac{1}{1+(\omega\tau)^{2(1-\alpha)}}$$
$$\sigma_i = \sigma_i^{0} + \Delta\sigma \frac{(\omega\tau)^{2(1-\alpha)}}{1+(\omega\tau)^{2(1-\alpha)}} \quad (7)$$

ω and τ are the circular frequency of the field and the time constant of the cytoplasmic dispersion, respectively. ε_i^{∞}, $\Delta\varepsilon$, σ_i^{0} and $\Delta\sigma$ are the relative permittivity at infinitely high frequency, the dielectric decrement as well as the cytoplasmic conductivity at low frequency and the conductivity increase resulting from the dispersion, respectively (see Table 1). Two cases for the dispersion width α have been considered, $\alpha=0$ and $\alpha=0.5$ [19].

5.2. Effect of the temperature on the ER peaks

A moderate temperature increase led to a linear increase of the ER peak frequencies f_{c1} and f_{c2} accompanied by an increase in the rotation peaks R_1 and R_2. This behavior was reflected by the theoretical ER spectra calculated from the parameters of Table 1. These results confirm previous ER experiments without temperature control [1,3,6,8]. The largest contribution to the temperature dependence of the peak magnitudes arose from the viscosity (Eq. (1)). The agreement of theory with experiment could be improved by introducing the cytoplasmic dispersion given by Eq. (7) especially for the 20 °C and 25 °C data [3]. However, Eq. (4) predicted higher R_1 and R_2 rotation peaks than experimentally found. To fit the points a scaling factor was introduced to account for the additional friction in the vicinity of the chip surface. A factor of 2.6 was used for all temperatures and conductivities.

Different effects may be taken into account to explain the remaining deviations in the rotation speed. The hydrodynamic friction coefficient for the biconcave cell rotating in the vicinity of the surface is not known (please also see theory section). In practice, the friction with the glass surface will depend on the surface distance and the shape of the cell. Both parameters depend on temperature and ionic strength, i.e. the external conductivity. For example, a more discocyte-shape, like it was observed at low conductivities, will give rise to an increase in the cell surface facing the chip and a subsequent increase in friction.

Furthermore, changes in the ionic cell state prior to and during the measurements will alter the electric cell properties and, subsequently, the induced torque. Ionic state changes are very complex and depend on the measuring solutions. They can hardly be fully controlled [20]. To reduce the effect of such changes no measurements later than 5 min after suspension were conducted.

Experimentally, a decrease in the first rotation peaks was found at a conductivity of 0.5 S/m for temperatures above 25 °C. Generally, the cell volume was increased in the medium conductivities range (microscopic observation). Volume changes may be related to a membrane phase transition resulting in a greater efficiency of water diffusion through the membrane [13]. This diffusion is related to the status of the membrane lipids in the classical view. Diffusion is more efficient when the membrane lipids are in their fluidic and not the gel state. Volume alterations will alter the ionic, water, and protein concentrations in the cytoplasm as well as the hindrance factor of the ionic mobility [20]. Theoretically, a volume increase may therefore result in an increase or decrease of the cytoplasmic conductivity.

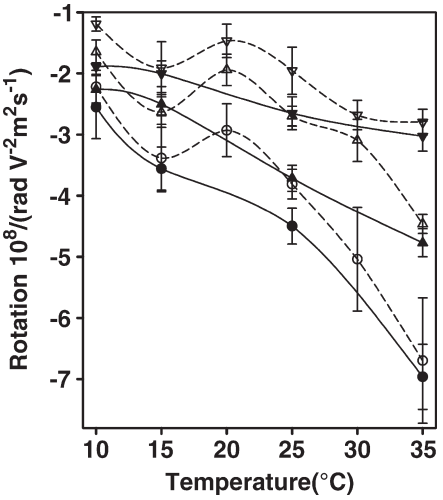

Fig. 5. First rotation peak at different selected temperatures for control (open symbols, dashed lines) and DIDS treated (filled symbols, solid lines) cells. The circles, triangles up and triangles down represent external conductivities of 0.02 S/m, 0.20 S/m and 0.40 S/m, respectively.

We found that the first characteristic frequencies differ by a factor larger than four at the very low external conductivities. An even larger frequency deviation was observed above 1 S/m at temperatures above 30 °C (Fig. 3A). This is much larger than theoretically predicted. Alterations in the membrane capacitance have a pronounced effect on the first characteristic frequencies. Nevertheless, the explanation of the temperature effect at low conductivities by a corresponding decrease in the membrane capacitance would require unrealistic transitions in the molecular membrane structure.

In striking contrast to our results, Bao et al. [22] described a strong increase of the membrane capacitance by a factor of about two with temperature in the range from 25 °C to 35 °C. Our results suggest a decrease by a factor of about four. An explanation for the strong spreading of our characteristic frequencies will probably require a combination of different effects, e.g. an increase in the cytoplasmic and membrane conductivities and a decrease in the membrane capacitance with temperature and frequency.

5.3. Membrane properties: the anomalous rotation speed at 15 °C

Another interesting result is an anomalous increase in the rotation speed at a temperature of 15 °C (Fig. 4A). This effect vanishes at 10 °C and temperatures above 20 °C in the medium and high conductivity ranges. Interestingly, the anomalous rotation corresponds to data on the transmembrane-transport rate of ions changing just around 15 °C [12,20]. Brahm [12] described a deflection point in the Arrhenius plot of the anion transport at 15 °C. The point was persistent even after partial band 3 inhibition by DIDS. Different explanations for this behavior were proposed. Either the energy barrier of chloride transport decreases at a critical temperature, e.g. due to phase transitions of some membrane components or the chloride exchange is rate limited by different rate limiting steps in the transport process below and above 15 °C. According to Brahm [12], the rate limiting step above 15 °C would possess a somewhat lower activation energy.

Probably, the transmembrane-mobility of anions is the major contribution to the AC-membrane conductance in HRBCs [7]. Nevertheless, the interpretation of our results by alterations in the membrane conductance requires the assumption of a more complex behavior of the membrane conductance with a minimum around 15 °C. A possible explanation was given by Prof. I. Bernhardt (personal communication) who proposed that the increase in the membrane conductance below 15 °C is due to the enhanced cation exchange at low temperatures (compare to [21]). Our results with DIDS are hinting at a large role of band 3 in these processes. DIDS-treatment increased the rotation speed at the first peak at various conductivities and temperatures (Fig. 5). This DIDS-induced increase in the rotation speed resulted in an alignment of all measuring points with those measured for the control at 15 °C. These results are in line with a decrease in the membrane conductance as described before [7,17]. These authors assume a decrease from 250 S/m^2 to 20 S/m^2 after DIDS inhibition of band 3 leading to an increase in rotation speed by about 32% at 5 mS/m [7]. The assumption of a membrane conductance of 20 S/m^2 (dashed line in Fig. 4A) could help explaining the anomalously high rotation speed of the control cells at 15 °C.

6. Conclusions

ER could be demonstrated to be an elegant method for detecting the temperature dependence of the electric HRBC parameters at the single cell level. Our experimental data could only roughly be fitted by our model assuming the standard temperature coefficients for all media. Our major findings are as follows:

(1) The anomalously high rotation speed at the first peak at 15 °C and the DIDS-effects on the rotation speeds for all other temperatures, hint at a major role of the band 3 protein for the membrane conductance.
(2) A temperature-spreading of the first characteristic frequencies much wider than that predicted for standard temperature coefficients of the media was found. A corresponding change in the membrane capacitance seems to require unrealistic transitions in the molecular membrane structure. An explanation for this effect is still missing. It might include effects related to the capacitance of the protein areas in the membrane that probably possess a specific capacitance much higher (about 4.2 F/m^2) than those of the lipid areas (about 0.74 F/m^2; please see: [23]).
(3) A dramatic increase in the first characteristic frequencies above 3 S/m especially for temperatures above 30 °C was found. A possible explanation might be the dispersion of membrane protein polarization leading to a decrease of the membrane capacitance around 3 MHz as already proposed by us [3].

In summary, our results suggest that the interpretation of ER data requires special attention to the temperature. Further, it is important to take cell shape changes induced by different suspension conditions into account. Temperature dependent ER measurements on the HRBC model system may lead to a better understanding of the electric cytoplasm and membrane properties of biological cells.

Acknowledgements

J.S. and D.W. are grateful for a stipend of the Prince of Songkla University and a financial contribution from project number StSch 2002 0418A of the Bundesamt für Strahlenschutz to J.G., respectively. The authors are grateful to the International Postgraduate Programme (IPP) supported by DAAD, BMBF and DFG. J. Donath is acknowledged for excellent technical assistance.

References

[1] J. Gimsa, P. Marszalek, U. Loewe, T.Y. Tsong, Dielectrophoresis and electrorotation of neurospora slime and murine myeloma cells, Biophys. J. 60 (1990) 749–760.

[2] S. Lippert, J. Gimsa, High resolution measurements of dielectric cell properties by a combination of AC-electrokinetic effects, in: P. Kostarakis (Ed.), Proceedings of the 2nd International Workshop on Biological Effects of EMFs, Rhodes, Greece, 2002, pp. 830–836.
[3] J. Gimsa, T. Mueller, T. Schnelle, G. Fuhr, Dielectric spectroscopic of single human erythrocytes at physiological ionic strength: Dispersion of cytoplasm, Biophys. J. 71 (1996) 495–506.
[4] W.M. Arnold, U. Zimmermann, Rotating-field-induced rotation and measurement of the membrane capacitance of single mesophyll cells of *Avena sativa*, Z. Naturforsch. 37 (1982) 908–915.
[5] J. Gimsa, D. Wachner, A polarization model overcoming the geometric restrictions of the Laplace solution for spheroidal cells: Obtaining new equation for field-induced forces and transmembrane potential, Biophys. J. 77 (1999) 1316–1326.
[6] R. Glaser, G. Fuhr, J. Gimsa, Rotation of erythrocytes, plant cells and protoplasts in an outside rotating electric field, Stud. Biophys. 96 (1983) 11–20.
[7] E. Donath, M. Egger, Dielectric behavior of the anion-exchange protein of human red blood cells: Theoretical analysis and comparison to electrorotation data, Bioelectrochem. Bioenerg. 23 (1990) 337–360.
[8] J. Sudsiri, D. Wachner, J. Donath, J. Gimsa, Can molecular properties of human red blood cells be accessed by electrorotation? Songklanakarin, J. Sci. Technol. 24 (2002) 785–789.
[9] M. Simeonova, D. Wachner, J. Gimsa, Cellular absorption of electric field energy: the influence of molecular properties of the cytoplasm, Bioelectrochemistry 56 (2002) 215–218.
[10] J.O.'M. Bockris, I. Reddy, K.N. Amulya, Modern Electrochemistry, 2nd edition, Plenum Publishing Corporation, New York, 1973.
[11] D.R. Lide, CRC Handbook of Chemistry and Physics, 74th edition, CRC press, Boca Raton, 1993.
[12] J. Brahm, Temperature-dependent changes of chloride transport kinetics in human red cells, J. Gen. Physiol. 70 (1977) 283–306.
[13] J.Z. Bao, C.C. Davis, R.E. Schmukler, Frequency domain impedance measurement of erythocytes: Constant phase angle impedance characteristics and a phase transition, Biophys. J. 61 (1992) 1427–1434.
[14] W.A. Wegener, V.J. Koester, R.M. Dowben, A general ellipsoid cannot always serve as a model for the rotational diffusion of arbitrarily shaped rigid molecules, Proc. Natl. Acad. Sci. U. S. A. 76 (1979) 635–636.
[15] K. Maswiwat, M. Holtappels, J. Gimsa, On the field distribution in electrorotation chambers: influence of electrode shapes, Electrochim. Acta (in press).
[16] J. Gimsa, E. Donath, R. Glaser, Evaluation of the data of simple cells by electrorotation using square-topped fields, Bioelectrochem. Bioenerg. 19 (1988) 389–396.
[17] R. Georgiewa, E. Donath, J. Gimsa, U. Loewe, R. Glaser, AC-field-induced KCl leakage from human red cells at low ionic strengths: Implication for electrorotation measurements, Bioelectrochem. Bioenerg. 22 (1989) 255–270.
[18] D. Mietchen, T. Schnelle, T. Mueller, R. Hagedorn, G. Fuhr, Automated dielectric single cell spectroscopy-temperature dependence of electrorotation, J. Phys., D, Appl. Phys. 35 (2002) 1258–1270.
[19] H. Pauly, H.P. Schwan, Dielectric properties and ion mobility in erythrocytes, Biophys. J. 6 (1966) 621–639.
[20] J. Gimsa, Th. Schnelle, G. Zechel, R. Glaser, Dielectric spectroscopy of human erythrocytes: investigations under the influence of nystatin, Biophys. J. 66 (1994) 1244–1253.
[21] A.L. Harris, CC. Guthe, F. Van't Veer, D.F. Bohr, Temperature dependence and bi-directional cation fluxes in red blood cells from spontaneously hypertensive rats, Hypertension 6 (1984) 42–48.
[22] J.Z. Bao, C.C. Davis, M.L. Swicord, Microwave dielectric measurements of erythrocyte suspensions, Biophys. J. 66 (1994) 2173–2180.
[23] J. Gimsa, Mechanisms of energy absorption at the cellular level: A first approach, Proceedings of the COST 244 BIS Conference on "Biomedical Effects of Electromagnetic Fields", Technical Univ., Munich, 2000, pp. 101–114, http://www.cost281.org/download.php?fid=231.